Prepared for submission to JINST

22nd International Workshop on Radiation Imaging Detectors

June 27, 2021 to July 1, 2021

Online

A Miniaturized Radiation Monitor for Continuous Dosimetry and Particle Identification in Space

St. Gohl,[a,d] **M. Malich,**[a] **B. Bergmann**[a] **P. Burian**[a,e] **C. Granja**[b] **E. Heijne**[a,f] **M. Holik**[a,e] **J. Jacubek**[b] **J. Janecek**[a] **L. Marek**[b] **C. Oancea**[b] **M. Petro**[a] **S. Pospisil**[a] **A. Smetana**[a] **P. Soukup**[b] **D. Turecek**[b] **and M. Vuolo**[c]

[a] *Institute of Experimental and Applied Physics, Czech Technical University in Prague, Husova 5, 11000 Prague Czech Republic*

[b] *ADVACAM, U Pergamenky 12, Prague, Czech Republic*

[c] *European Space Agency - European Space Research and Technology Centre, 2200 AG Noordwijk, The Netherlands*

[d] *Department of Surface and Plasma Science, Faculty of Mathematics and Physics, Charles University, V Holesovickach 2, Prague, Czech Republic*

[e] *Research and Innovation Centre for Electrical Engineering, University of West Bohemia, Univerzitni 26, 30100 Pilsen, Czech Republic*

[f] *CERN, Esplanade des Particules 1, 1211 Geneva 23, Switzerland*

E-mail: Stefan.gohl@utef.cvut.cz

Abstract: A Miniaturized Radiation Monitor (MIRAM) has been developed for the continuous measurement of the radiation field composition and ionizing dose rates in near earth orbits. Compared to currently used radiation monitors, the presented device has an order of magnitude lower weight while being comparable in power consumption and functionality. MIRAM is capable of on-board real-time self-diagnostic. Furthermore, it supports on-board analysis of the measured data to be able to work autonomously. The dose rate is calculated continuously based on the energy deposition in the Timepix3 detector. For the estimation of the particle species composition of the radiation environment, two methods are applied depending on the current flux. At lower fluxes ($< 10^4$ particles per cm^2 per s), a track-by-track analysis based on temporal coincidence is applied. At higher fluxes, a less power and memory consuming method is utilized. This method is using the averaged deposited energy per pixel to estimate the electron and proton content of the radiation field.

Keywords: Radiation monitoring, Solid state detectors, On-board space electronics, dE/dx detectors, Particle tracking detector

[1]Corresponding author.

Contents

1 Introduction **1**

2 Hardware Features **1**

3 Firmware Features **2**

4 Modes of Operation **4**

4.1 Method A 5

4.2 Method B 6

5 Conclusion **7**

1 Introduction

Space radiation poses a threat not only to human space flight missions, but also to the electronic equipment of any space mission (eg. [1, 2]). Some dramatic space system failures and disturbances in recent years have been assumed to be radiation-induced malfunction of critical electronics parts. The space radiation environment consist of a variety of particle species, including electrons, protons and heavy ions, which may pose threats at different levels to different electronic devices. Therefore, the presence of a radiation monitor on-board of any mission is highly desirable to provide the capability to take protective measures in-flight and to contribute with flight-data to the improvement of existing radiation environment models. This paper describes the development of a novel Miniaturized Radiation Monitor (MIRAM) for this purpose. It was developed by the Institute of Experimental and Applied Physics (IEAP) and ADVACAM under the supervision of the European Space Agency (ESA). Compared to the currently used devices [3, 4], has lower weight and power consumption. It is capable of providing a continuous measurement of dose as well as an estimation of the particle species composition of the radiation environment.

2 Hardware Features

MIRAM sits in a aluminium casing with the dimensions 80 x 60 x 30 mm. Its nominal power consumption is 1.2 W with a peak consumption of 1.8 W. MIRAM is divided into two parts - the low power circuit (LPC) and the Acquisition and Processing Module (ACQP). The LPC is based on four single pad diodes. This part controls the duty cycle of MIRAM. It is responsible for data handling. The ACQP part is a medium-power consuming part that features a Timepix3 [5], which is the center piece of the MIRAM device. Timepix3 is a hybrid pixel detector developed by the Medipix3 collaboration[1]. The detector consists of a sensor layer flip-chip bump-bonded to an ASIC[2].

[1] https://medipix.web.cern.ch/home

[2] Application specific integrated circuit

The sensor is divided into a square matrix of 256 x 256 pixels with 55 μm pixel pinch. Timepix3 provides the ability to simultaneously measure per pixel energy and time (time granularity: 1.56 ns) in a data-driven (self-triggered) readout mode with hit rates up to 40 Mhits s^{-1} cm^{-2}. Higher fluxes can be measured using the frame based mode.

The architecture of MIRAM can be seen in Figure 1. The MIRAM box itself is shown in Figure 2 in a closed configuration and in Figure 3 the inside is depicted.

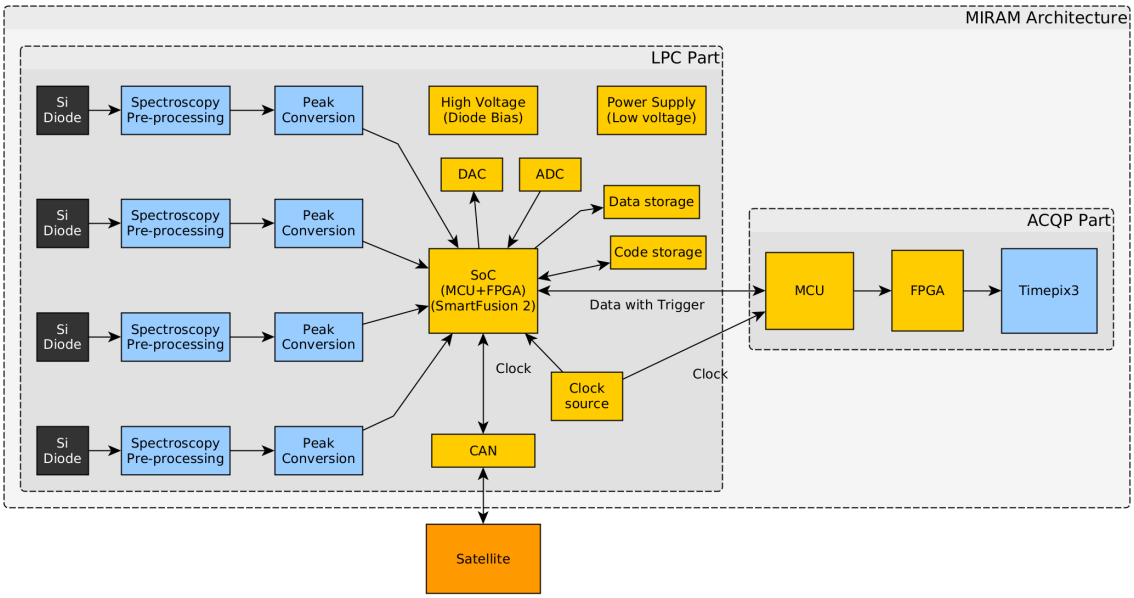


Figure 1. Scheme of the MIRAM architecture with the LPC part on the left and the ACQP part on the right.

The diodes and Timepix3 are separated by a 7 mm thick aluminium electron filter. The sensor material of diodes and the Timepix3 is Si. The sensor thickness comes with two alternatives, either 300 μm or 500 μm. The diodes always have the same thickness as the sensor. The electronic parts are low-power consuming and radiation tolerant commercial off-the-shelf components. The device further features a high-voltage power supply, 4 MB data storage M-RAM with an optional 16 MB DRAM and a CAN interface for communication with the satellite. Additionally, MIRAM has the capability of on-board real-time self-diagnostic as well as on-board analysis, which is subject of the Section 4.

3 Firmware Features

MIRAMs Firmware is based on FreeRTOS (Real-time operating system for micro controllers). FreeRTOS provides a standard OS mechanisms - queues, mutex, semaphores etc. The virtual memory address space called VirtualRegisterMap (VRM) was established for the internal storing of the data products and detector configuration. The external device (superior system) can access (reading and writing values of registers) to VRM via CAN bus. The LPC firmware divides the complex functionality into several separated simpler tasks, as depicted in Figure 4. The individual functionalities shall be explained in the following.

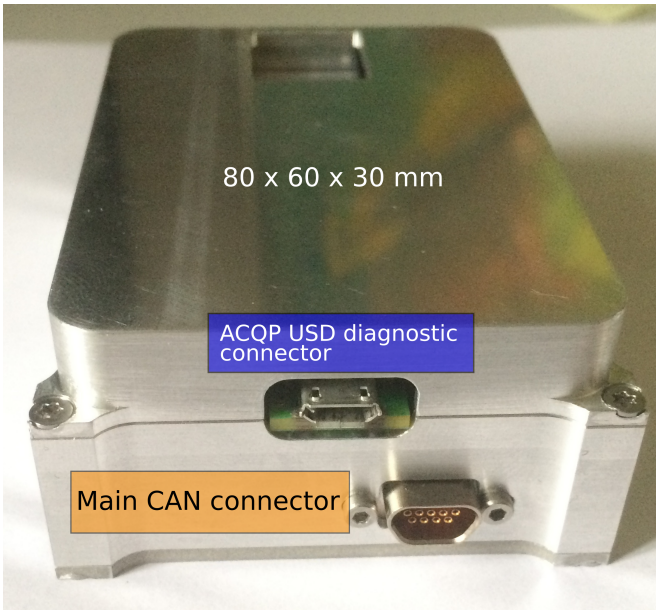


Figure 2. MIRAM in aluminum housing with upper MicroUSB (Diagnostic) and bottom MicroD (Main satellite) connectors.

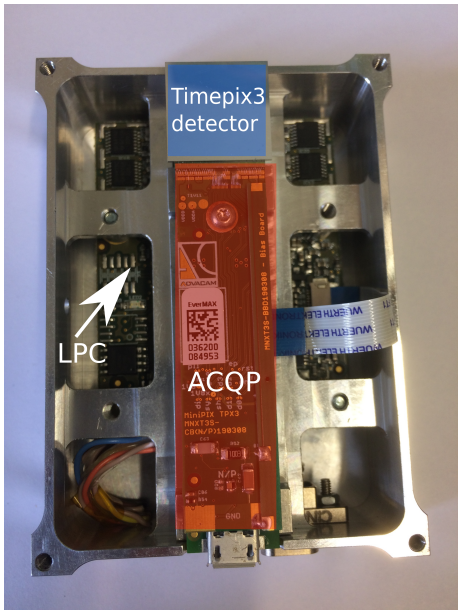


Figure 3. MIRAM detail view from inside: ACQP with Timepix3 chip on top, LPC on bottom.

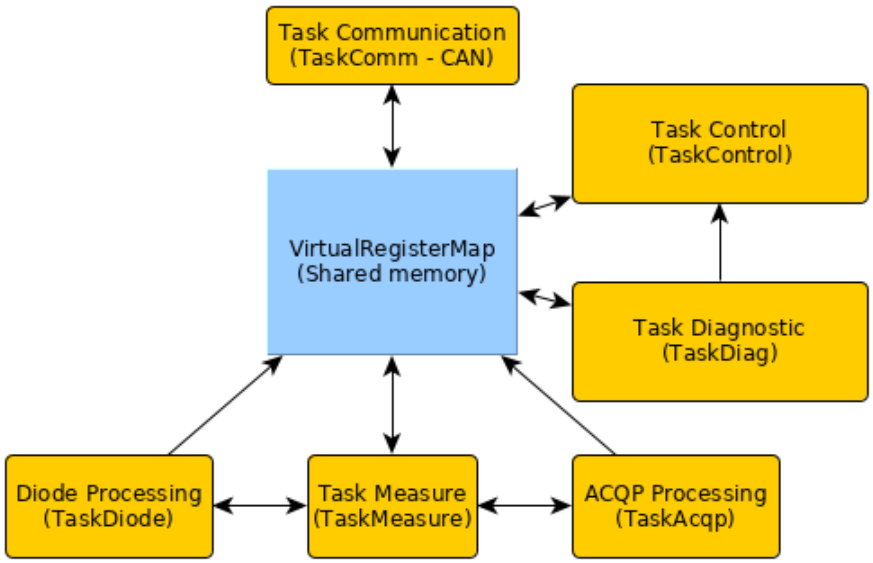


Figure 4. Schematic architecture of MIRAM firmware.

TaskControl - This unit provide a virtual register map functionality. All status information of the system, applicable run time parameters and device settings are located in the VRM. All settings and status information can be accessed externally via a unified interface. It significantly simplifies a possible future integration of MIRAM into complex set-ups. A validation of external user access requests are performed in order to reject the application of an invalid configuration that may cause

incorrect behavior of the device.

TaskComm - The unit handles low level communication over the CAN communication bus with the satellite.

TaskMeassure - This unit primarily performs an automated data product download. Depending on the user configuration, selected data product components can be obtained without further requests. Transmission of data products can be initiated automatically if the appropriate event trigger or time period trigger is configured. The second objective of the unit is to supervise the execution of acquisition procedures performed in the scope of the subordinate two units *TaskAcqp* and *TaskDiode*.

TaskDiode - This unit is responsible for the energy readout of the diodes. The events are stored in the VRM memory.

TaskAcqp - The unit provides internal SPI communication between the ACQP module and the LPC. It manages the ACQP operations (Timepix3), especially the data acquisition. Partial results will be downloaded from the ACQP module and stored to the VRM memory.

TaskDiag - The unit is responsible for a common diagnostic functionality (e.g. Single Error Correction Double Error Detection (SEDEC) and Watchdog Timer (WDT)). It monitors the SEDEC unit to detect and correct Single Effect Upset (SEU) in the LPC part. Additionally, the unit regularly resets the WDT to prevent it from counting down to zero. If the timer runs out, the WDT resets the entire system to autonomously recover from faults.

4 Modes of Operation

MIRAM has two operation modes, one for high fluxes, labelled Method A, and one for low fluxes, labelled Method B. The reason for having two methods is that the power consumption, mainly for the processing unit, would rise significantly with the amount of data produced. This is also true for the memory space. At higher fluxes, Timepix3 easily produces GB of data within a few minutes. A method is needed that handles large amount of data quickly and without the need for much processing.

Roughly speaking, Method A provides a rough estimation of electron and proton content in the radiation field. It does not analyse each individual track, but has a lower power consumption. Method B has a higher power consumption, but is an event by event analysis. The identification of events is based on the time response on the pixel level. The transition between the two methods appears at 10^3 - 10^4 particles per cm^2 per second. The transition depends on the memory usage rather than the exact flux. Both methods provide information on the dose-rate, individual particle fluxes for electron, protons and ions (ions only in the case of Method B) and the spectrum of deposited energy.

The development was supported by a Monte Carlo simulation conducted with Geant4 [6]. The model was converted from the STL format, which is commonly used in computer-aided manufacturing, to the GDML format. GDML is readable by Geant4 and therefore, the model could be implemented in the simulation with high detail. The detector model implemented in the simulation was validated with measured proton and electron data. Additionally, performance tests were conducted by simulating realistic space environments in several orbits. These results are not shown here as they go beyond the scope of this paper.

4.1 Method A

Method A was designed to give an estimation of the electron and proton flux without using a lot of computing power and memory. It was developed with the help of the simulation and tested on real space data from the Space Application of Timepix based Radiation Monitor (SATRAM) [7, 8]. SATRAM is attached to the Proba-V satellite and features the first Timepix [9] exposed to outer space.

The strategy is to sum up the deposited energy in the detector over a few hundreds of milliseconds and divide it by the number of pixel hits of all pixels within this time window. A simulation was conducted with the MIRAM setup simulating electrons and protons. To start with, a small number of purely electrons were simulated hitting the detector, to imitate low fluxes. While keeping the total number of particles constant, 5% of the electrons were step by step converted repeatedly into protons until there were only protons. Then the number of total particles were increased and the procedure just described was executed again. This was repeated until there were a few hundred thousand particles in the detector.

The result can be seen in Figure 5. It shows, that for sufficiently high number of hit pixels, the energy per pixel only varies very little around a constant value for each particle composition. The particle composition with a 100% of electrons has the lowest value of energy per pixel, while a 100% protons has the highest value of energy per pixel.

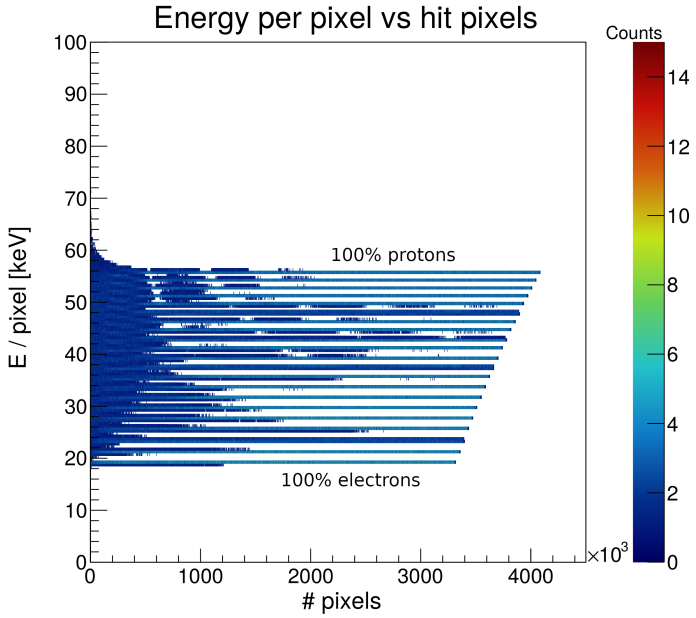


Figure 5. Simulation of energy per pixel compared to the number of hit pixels. The particle composition of a 100% of electrons corresponds to the lowest number of energy per pixel, while 100% of protons corresponds to the highest number of energy per pixel. For sufficiently high number of hit pixels, the energy per pixel is nearly constant.

The fact that the energy per pixel only depends on the particle composition makes it possible for Method A to give an estimation on particle species composition while using less resources. It only has to sum up the deposited energy, divide it by the number of pixel hits and compare it with

a look-up table. This table was created by combining measurements with a Timepix3 on Earth and the simulation. The measurements were done in several facilities providing proton and electron beams of various energies.

Furthermore, this method was tested on SATRAM data. The comparison is presented in Figure 6. The blue points represent the measured data, while the red points are simulations of specific particle compositions. Towards higher number of pixel hits the data is splitting into two branches. Unlike in the simulation before, the energy per pixel is not constant, but rises with higher pixel hit counts. The maximum of pixel hits is just above 60k pixels, while the energy per pixel can still rise. The reason for that is that SATRAM feature a Timepix detector, the predecessor of Timepix3. Timepix is not capable of counting more than one pixel hit per pixel while more energy can be deposited in one time window.

In Figure 6 the simulation for 100% electrons, corresponding to the lower branch, and for 85% electrons and 15% protons, corresponding to the upper branch, has been overplotted on top of the measurement data. This has been found to be the best match between the simulated data and the branches in the measurement. At lower pixel hit counts (<20k hit pixels), the distribution of energy per pixel varies much more, showing that Method A is not suitable for low fluxes. Data from the upper branch has been located to be in the South Atlantic Anomaly, while the lower branch was located in the polar region as illustrated in Figure 7.

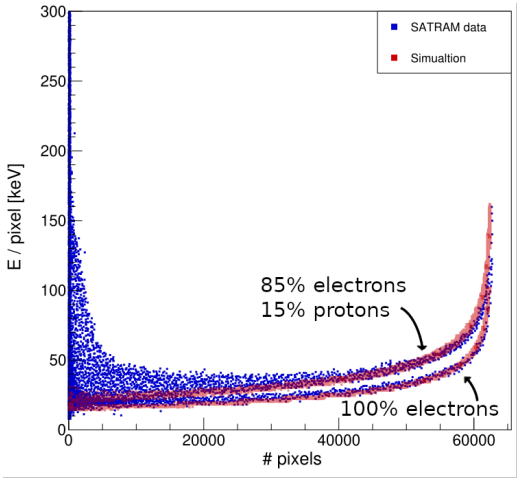


Figure 6. Matching measurement (blue) and simulation (red) of energy per pixel in relation to pixel hits for SATRAM. The simulation for 100% electrons and 85% electrons and 15% protons matches best the data for higher number of pixel hits (> 40k). See text for further explanation.

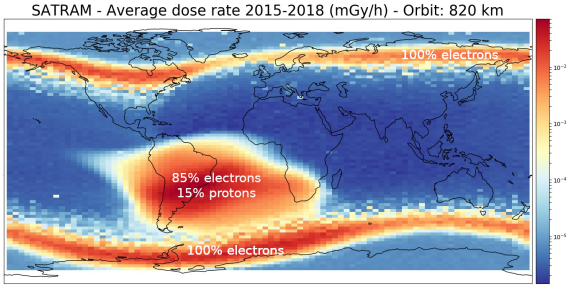


Figure 7. Average dose rate measured by SATRAM during the years 2015 to 2018. The proton and electron composition estimated by Method A is indicated for the South Atlantic Anomaly and the polar regions.

4.2 Method B

Method B is more suitable for situations with low fluxes, when an event by event based analysis does not need too much computing power. The identification of particle tracks is done through

temporal coincidences as illustrated in Figure 8. Pixels that are hit consecutively in a very short period of time are considered to contribute to the same event. Larger gaps between the pixel hits within the sampling time window leads to the identification of another event.

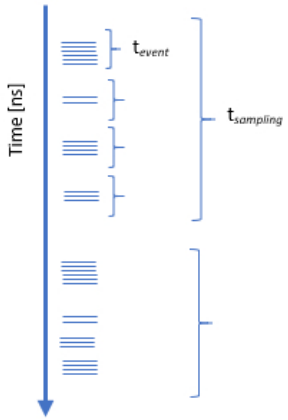


Figure 8. Schematic depiction of event sampling through temporal coincidence. Signals with a timestamp close to each other are identified as a single event.

The next step is to sort the pixels into low, medium and high values of energy and sum up the energy in each category. Low energy pixels are below 31 keV per pixel and high energy pixel are above 173 keV per pixel with the medium pixel having energies between those values. The distribution of these three values covers a three dimensional space as depicted in Figure 9. Each particle species occupies a certain area in this space. Figure 9 shows data from measured electrons (red), protons (blue) and ions (green) sorted into the three categories. Here, the low, medium and high values are labelled E_I, E_{II} and E_{III}, respectively. The data shown are from measurements on Earth and serve as database for Method B. Additionally, an unknown state X is depicted in Figure 9. Method B estimates the probability of the event X being of a certain species according to the surrounding data points as demonstrated by the numbers in the bottom right of Figure 9. In this case, it would clearly be an ion. Electrons mostly have a non-zero value only in E_I. Protons exist mostly in the E_I-E_{II} plane with values in E_{III} below 1 MeV, while ions show often values above 1 MeV in E_{III}.

5 Conclusion

A low power, low mass device for in orbit particle detection (MIRAM) was developed. It features the Timepix3 detector technology with a Si sensor of either 300 μm or 500 μm thickness. Timepix3 is supported by four Si diodes of the same thickness. Furthermore, the device is capable of on-board data processing. Its nominal power consumption is 1.2 W with a peak consumption of 1.8 W. With its mass just below 150 g it is smaller and lighter than present-day radiation monitors (SREM: 2.4 kg, ICARE: 2 kg). The components have a radiation tolerance of at least 100 krad. MIRAM will serve as a dosimeter, particle rate meter and providing particle separation capability.

The device employs two methods to handle the data depending on the flux. For high fluxes, Method A provides information about the electron and proton content of the radiation field based on the averaged deposited energy per pixel over a fixed time frame of a few 100 μs. This method guarantees a low power consumption at a high data rate (i.e. high fluxes). Method B provides a track-by-track analysis based the time response on pixel level. It has higher power and memory requirements for the processing unit, which is why it is used at lower fluxes. The transition depends primarily on the memory usage and occurs between 10^3 - 10^4 particles per cm^2 per second.

MIRAM was accepted for the GOMX5 cubesat mission, which is currently planned for 2022.

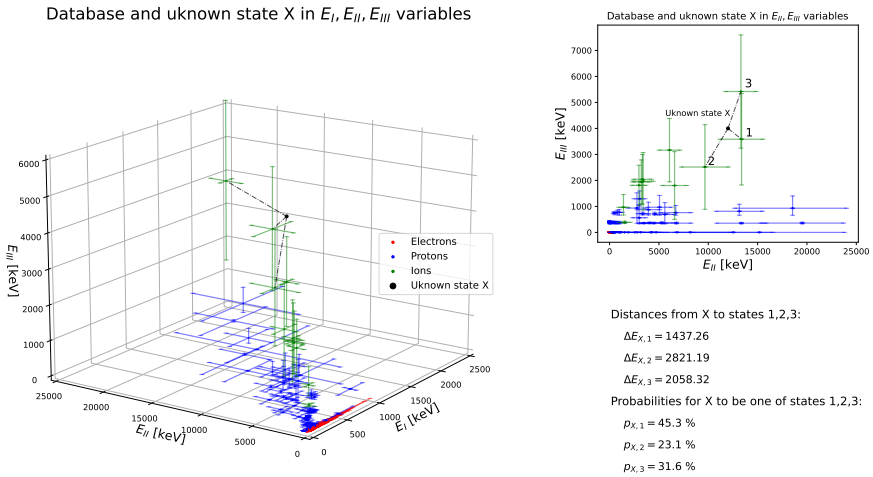


Figure 9. Depiction of the functionality of Method B. On the left, electrons (red), protons (blue) and ions (green) are shown in the 3-dimensional space that is defined by the sum of low energy pixels (E_I < 31 keV), medium energy pixels (E_{II}) and high energy pixels (E_{III} > 173 keV). On the top right, a projection on the E_{II}-E_{III} can be seen. An unknown event X is added to both diagrams. It's proximities to states 1, 2 and 3, and the probabilities for event X being a particle like either 1, 2 or 3, are shown on the bottom right. In this case, it is clearly an ion as all three states are ions.

Acknowledgments

The authors acknowledge funding from the European Space Agency (contract number: 4000122160/17/UK/ND).

References

[1] R. K. Tripathi, *Radiation effects in space*, in *Application Of Accelerators In Research And Industry: Twenty-First International Conference*, F. D. McDaniel and B. L. Doyle, eds., vol. 1336 of *AIP Conference Proceedings*, pp. 649–654, Univ N Texas; Sandia Natl Labs; Los Alamos Natl Lab; AccSys Technol Inc; High Voltage Engn Europa BV; Natl Electrostat Corp; TDK-Lambda Amer, 2011, DOI.

[2] J. Adams, D. Falconer and D. Fry, *The ionizing radiation environment in space and its effects*, in *Space Weather: The Space Radiation Environment*, Q. Hu, G. Li, G. Zank, X. Ao, O. Verkhoglyadova and J. Adams, eds., vol. 1500 of *AIP Conference Proceedings*, pp. 198–203, Univ Alabama, Ctr Space Plasma & Aeronom Res, 2012, DOI.

[3] D. Boscher, S. A. Bourdarie, D. Falguere, D. Lazaro, P. Bourdoux, T. Baldran et al., *In flight measurements of radiation environment on board the french satellite jason-2*, *IEEE Transactions on Nuclear Science* **58** (2011) 916.

[4] H. Evans, P. Bühler, W. Hajdas, E. Daly, P. Nieminen and A. Mohammadzadeh, *Results from esa srem monitors and comparison with existing radiation belt models*, *Adv. Space Res.* **42** (2008) 1527.

[5] T. Poikela, J. Plosila, T. Westerlund, M. Campbell, M. D. Gaspari, X. Llopart et al., *Timepix3: a 65k channel hybrid pixel readout chip with simultaneous toa/tot and sparse readout*, *J. Instr.* **9** (2014) .

[6] S. Agostinelli, J. Allison, K. Amako, J. Apostolakis, H. Araujo, P. Arce et al., *Geant4—a simulation toolkit*, *Nucl. Instrum. Methods A* **506** (2003) 250.

[7] S. Gohl, B. Bergmann, H. Evans, P. Nieminen, A. Owens and S. Pospisil, *Study of the radiation fields in leo with the space application of timepix radiation monitor (satram)*, *Adv. Space Res.* **63** (2019) 1645.

[8] C. Granja, S. Polansky, Z. Vykydal, S. Pospíšil, A. Owens, Z. Kozacek et al., *The satram timepix spacecraft payload in open space on board the proba-v satellite for wide range radiation monitoring in leo orbit*, *Planet. Space Sci.* **125** (2016) 114.

[9] X. Llopart, R. Ballabriga, M. Campbell, L. Tlustos and W. Wong, *Timepix, a 65k programmable pixel readout chip for arrival time, energy and/or photon counting measurements*, *Nucl. Instrum. Methods A* **581** (2007) 485.